KSCE Journal of Civil Engineering (2020) 24(4):1070-1082
DOI 10.1007/s12205-020-0216-x

pISSN 1226-7988, eISSN 1976-3808
www.springer.com/12205

Geotechnical Engineering

Liquefaction Potential Assessment of Brahmaputra Sand Based on Regular and Irregular Excitations Using Stress-Controlled Cyclic Triaxial Test

Shiv Shankar Kumar[a], **Arindam Dey**[b], **and A. Murali Krishna**[c]

[a]*Dept. of Civil Engineering, National Institute of Technology Patna, Patna 800005, India*
[b]*Dept. of Civil Engineering, Indian Institute of Technology Guwahati, Guwahati 781039, India*
[c]*Dept. of Civil Engineering, Indian Institute of Technology Tirupati, Tirupati 517506, India*

ARTICLE HISTORY

Received 26 February 2019
Revised 23 September 2019
Accepted 28 January 2020
Published Online 11 March 2020

KEYWORDS

Liquefaction
Irregular and regular excitation
Shear strain accumulation
Excess pore-water pressure
Cyclic triaxial test
Brahmaputra sand

ABSTRACT

The response of saturated soil during earthquakes is governed by many factors such as frequency content, strain, stress, excess pore-water pressure and strength variations within the soil mass. This paper highlights the effect of strains on the stiffness modulus and its degradation at the liquefied condition of cohesionless soil. Cyclic triaxial (CT) tests, in stress-controlled manner, were carried out on saturated sandy soil specimens made at different relative density (D_r = 30% – 90%) and effective stress (σ'_c = 50 – 200 kPa). The reconstituted specimens were subjected to regular and irregular stress histories. Representative strong motions with varying PGA were chosen, and the corresponding irregular stress histories were used. Additionally, regular stress histories constituted from different cyclic stress amplitudes were also used. The responses of the saturated specimen were obtained in terms of the excess pore-water pressure generation and strain accumulation with elapsed time. In comparison to the standard frequency and duration parameters (namely the predominant period and significant durations), it is observed that the responses are more influenced by Arias intensity and specific energy density of the strong motion. Based on the increase in pore-water pressure, reduction in shear modulus and increase in shear strain within the specimens, the complete manifestation of liquefaction is divided in four zones, namely the no liquefaction zone, quasi-liquefaction zone, zone marking the onset of liquefaction and the completely liquefied zone. The criteria for the onset of liquefaction of Brahmaputra sand involving shear strain, peak ground acceleration and cyclic stress ratio are provided.

1. Introduction

The behaviour of soils during the earthquakes is governed by the excitation level (in terms of peak ground acceleration (PGA)) and the position of water table location (which controls the saturation/unsaturation condition of soil). Based on the dynamic response, it is well established that the saturated silty sands are highly prone towards liquefaction (Seed and Idriss, 1971; Hardin and Drnevich, 1972; Iwasaki et al., 1978; Kokusho et al., 1982; Seed et al., 1986; Chung et al., 1984). As the particle size distribution and fine content present in the sands vary in the regional sands, the responses of saturated silty sands of different regions exhibit unique behaviour when subjected to regular or irregular seismic motions. Saturated soils, when subjected to a dynamic excitation, exhibit rise of the excess pore-water pressure (PWP), resulting in the reduction of strain-dependent shear strength. Under extreme conditions, when the applied stresses or accumulated strains become greater than the permissible levels, liquefaction and its associated damages are manifested (Vucetic and Dobry, 1991; Ishibashi and Zhang, 1993; Stokoe et al., 1995; Sitharam and Govindaraju, 2003). These studies made use of regular (sinusoidal) excitations as a simplistic representation of the actual irregular strong motion, which can be used as cyclic loading during experimental investigations. However, such simplifications can lead to largely different dynamic response, which are mostly used to identify the dynamic properties of soils (strain dependent shear modulus and damping ratio). On the other hand, the application of irregular seismic excitations would help in assessing the liquefaction of saturated soil specimens. Therefore, ascertaining the behaviour of saturated granular soils under irregular and

CORRESPONDENCE Arindam Dey arindamdeyiitg16@gmail.com Dept. of Civil Engineering, Indian Institute of Technology Guwahati, Guwahati 781039, India

regular excitations is of utmost importance.

Ishihara and Yasuda (1972, 1975) reported the liquefaction characteristics of saturated sandy soil using both irregular and regular excitations. It was suggested that in case of liquefaction potential evaluation using regular cyclic loading, 47 – 65% of the maximum shear stress (τ_{max}) of the irregular stress-time history should be applied for 20 loading cycles. Seed and Idriss (1971) emphasized that the number of regular loading cycles to initiate the liquefaction depends on the earthquake magnitude and its duration. In order to develop a suitable liquefaction criteria for sands, cyclic traxial (CT) tests were performed by several researchers using different testing conditions, seismic excitations, soil types, degree of saturation and initial in-situ stresses (Seed and Lee, 1966; Dobry et al., 1982; Vucetic and Dobry, 1991; Ladd et al., 1989; Ishihara, 1996; Lombardi et al., 2014). Researchers have used realistic earthquake time histories in triaxial testing of sandy soil specimens, and reported that the maximum shear strain (γ_{max}) required to initiate the liquefaction is close to 3.75% (Ishihara, 1996; Tsukamoto et al., 2004). From similar tests, the threshold volumetric shear strain (γ_t), required to initiate cyclic settlement of sand, was found in the range of 0.01 – 0.02% (Hsu and Vucetic, 2004). This threshold volumetric shear strain is a limiting value, below which the generation of excess PWP is insignificant (due to negligible sliding contacts between sand particles), and is not regulated by the initial density of the soil (Ladd et al., 1989). Based on strain-controlled cyclic tests, for saturated sandy soil, Kumar et al. (2015) were found that γ_t is in the range of 0.01 – 0.02%. Based on CT testing of partially saturated sandy soils, researchers have provided a correlation between cyclic shear strains (γ_c) and volumetric strains (Sawada et al., 2006), and reported that γ_c required to trigger the liquefaction, for clean sands, is in the range of 0.4 – 3% (Dobry et al., 2015; Dobry and Abdoun, 2015). For practical purposes, the consideration of γ_{max} = 3.75% and γ_t in the range 0.01 – 0.02% may not be always judicious for liquefaction related studies, due to their intricate dependency on particle size and prevailing site conditions.

Based on numerical studies, it is established that the alluvial basin of Brahmaputra river, North-eastern India, is susceptible to liquefaction (Basu et al., 2017). It is worth mentioning that this region of the country falls under the aegis of highest seismicity (as per IS 1893:2002). Hence, it becomes imperative to study the dynamic characteristic of regional Brahmaputra sand (BS). Based on CT tests, using regular and irregular seismic excitations, this article reports the threshold shear strain and cyclic shear strain of BS, and identifies its liquefaction potential. As liquefaction is generally reported in loose sand deposits at shallower depths, BS specimens were reconstituted at various relative densities (D_r = 30, 60 and 90%) and confining stresses (σ_c' = 50, 100, 150 and 200 kPa). For the experimental investigation, the specimens were subjected to regular excitation (1 Hz loading frequency, f, at cyclic stress ratio, CSR = 0.05, 0.1, 0.2 and 0.3) as well as irregular seismic excitations (the 1995 Kobe, the 2001 Bhuj and the 2012 Tezpur strong motions).

2. Study Region and Selection of Strong Ground Motions

Guwahati (26.18°N and 91.75°E) is the largest city of North-East

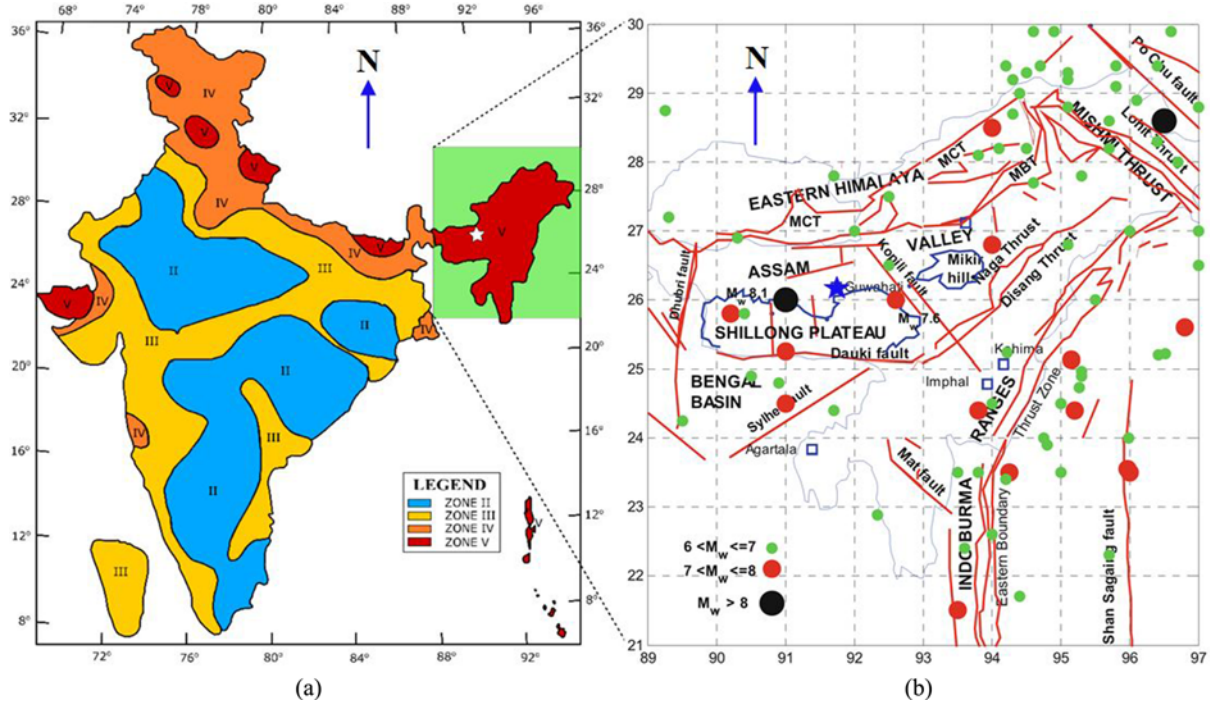

Fig. 1. Seismotectonic Map of India: (a) Seismicity of India and Study Region (IS-1893, 2002), (b) Details of Seismic Fault Nearby the Study Region (as per Raghukanth and Dash, 2010)

India (Fig. 1(a)). As shown in Fig. 1(b), this region is bounded by six major seismotectonic blocks (Raghukanth et al., 2008). Several earthquakes of varying intensities, moment magnitudes (M_w) ranging from M_w5 to M_w8.7, has been effective in this region. For $M_w > 8$, Nath et al. (2008) listed the average PGAs as 0.18 g, 0.23 g, 0.33 g, 0.50 g, and 0.82 g, for low, moderate, moderately high, high and very high seismic hazards zones, respectively. As per IS-1893 (2002), the entire North-East region of India comes under seismic zone V. Accordingly, for the maximum considered earthquake (MCE) and design basis earthquake (DBE) scenarios, the design PGAs are assessed as 0.36 g and 0.18 g, respectively. Thus, accounting the prevalent seismicity of the region, three different acceleration time histories (Bhuj, Tezpur and Kobe strong motions) with PGA ranging from 0.103 g to 0.834 g, is chosen to represent low, moderately high and very high seismic hazards.

3. Experimental Investigation

3.1 Soil Characterisation, Testing Apparatus and Sample Preparation

BS, used in this study, is collected from the Brahmaputra riverbed near Guwahati city. Fig. 2 depicts the particle size distribution of BS (as per ASTM D7928, 2017), and indicates that it is poorly graded (as per ASTM D2487, 2011) and highly prone to liquefaction as per standard criteria (Tsuchida, 1970; Ishihara et al., 1980; Xenaki and Athanasopoulos, 2003). The physical properties of BS are listed in Table 1. The specific gravity, the minimum and maximum dry unit weight of BS is obtained as 2.7, 13.85 kN/m^3 and 16.84 kN/m^3, respectively (as per ASTM D854 (2014), D4253 (2016), and D4254 (2016), respectively). Based on earlier findings (Kumar et al., 2018), Table 1 also lists the range of small-strain dynamic properties of the BS soil specimens of varying relative densities (30 – 90%) and subjected to varying confining pressure (50 – 200 kPa). The small-strain dynamic properties comprise shear wave velocity ($V_s = \sqrt{\frac{G_{max}}{\rho}}$, where ρ is the density of soil), maximum shear modulus (G_{max}) and the corresponding small-strain damping ratio (D_{min}).

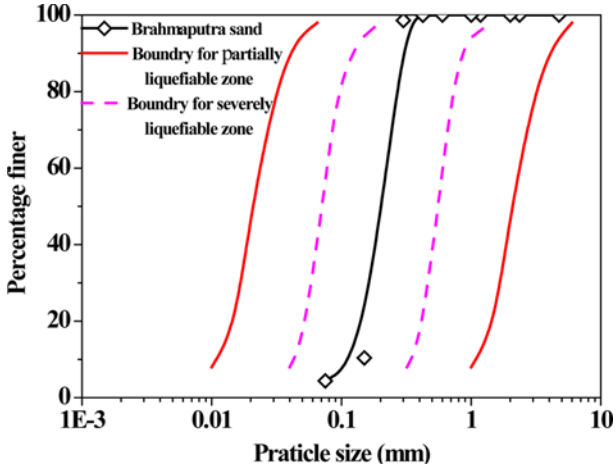

Fig. 2. Particle Size Distribution of Brahmaputra Sand

Table 1. Physical and Small-Strain Dynamic Properties of Brahmaputra Sand

Properties	Values
Mean grain size, D_{50} (mm)	0.21
Min.dry unit weight (kN/m^3)	13.85
Max.dry unit weight (kN/m^3)	16.84
Uniformity coefficient (C_u)	1.47
Coefficient of curvature (C_c)	1.09
Classification symbol	SP
Maximum shear modulus (G_{max}) (MPa)	~ 80 – 110
Small-strain Damping ratio (D_{min}) (%)	~ 0.6 – 1.1

The cyclic traxial tests were conducted in an automated testing apparatus, comprising a 100 kN loading frame of capacity and a pneumatically controlled dynamic actuator (0 – 30 mm operational displacement range and 0.01 – 10 Hz operational frequency range); further details about the apparatus are available in Kumar et al. (2017). Cylindrical BS samples (70 mm dia and 140 mm height) were prepared using dry pluviation technique (ASTM D5311. 2013). The saturation of the sample was achieved first by passing gaseous Carbon dioxide (CO_2) for 10 – 15 minutes, followed by flushing with de-aired water through incremental application of cell pressure (CP) and back pressure (BP), while maintaining a constant difference of 10 kPa. After every increase of CP, B-value (Skempton's pore-pressure parameter) was monitored, and the saturation process was stopped when $B = 0.98$ was achieved. For the present study, the same as achieved at BP = 200 kPa. After attaining the saturation, the specimen was isotropically consolidated to a targeted σ_c' by increasing CP, while maintaining a constant BP = 200 kPa. CP was increased in such a way that the difference between CP and pore pressure (this is the residual pore pressure at the end of consolidation, which is always slightly greater than BP) attains the targeted effective stress. After achieving a stabilized pore pressure generation, the drainage valve was opened to allow for complete drainage from the specimen that resulted in the decrease in volume and increase in the effective stress. At the end of consolidation, the effective stress is equal to the difference between CP and the residual pore pressure in the specimen. After achieving the desired effective stress, subsequent cyclic loading was applied. Further intricate details of the procedure are available in Kumar et al. (2017).

3.2 Irregular and Regular Seismic Excitations

In the present study, the regular excitations are referred to harmonic excitations having constant amplitude and a single frequency over the duration of the occurrence of motion. Such excitations are used in both strain-controlled and stress-controlled loadings. On the other hand, the irregular excitations are referred to those motions having varying amplitudes and frequencies during the occurrence of the motion. Such excitations are used to represent the stress-controlled loading in the present study.

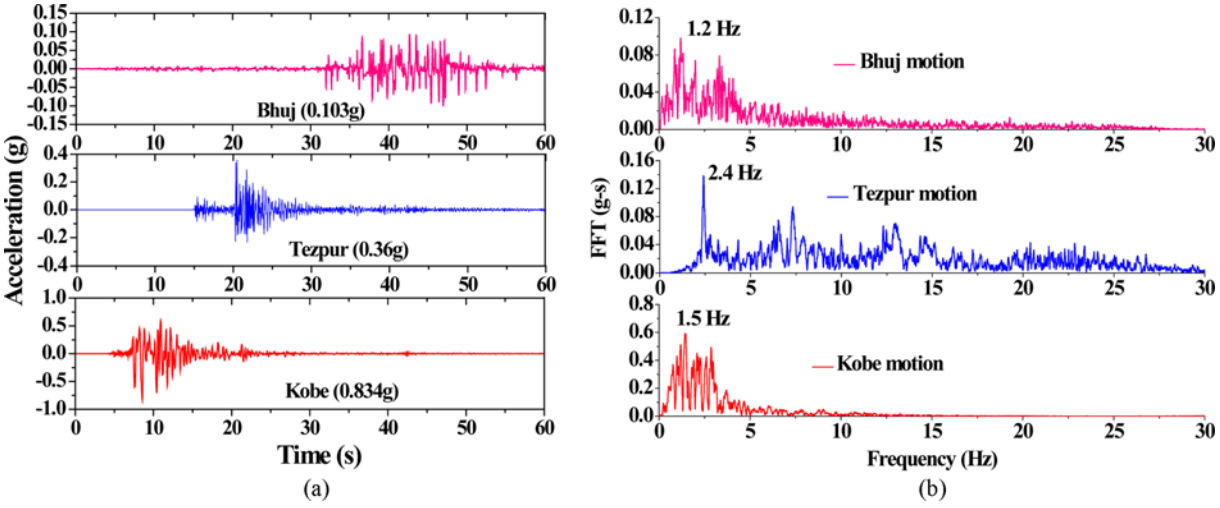

Fig. 3. Characteristics of the Chosen Strong Motions: (a) Acceleration-Time Histories, (b) Fourier Amplitude Spectra

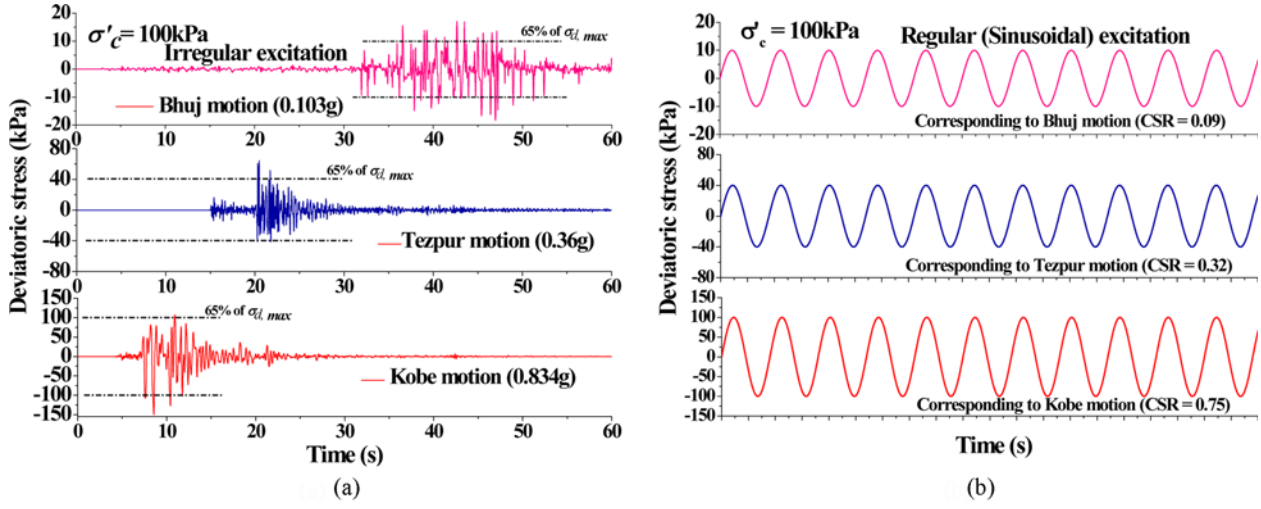

Fig. 4. Typical Variation of Deviator Stress at $\sigma_c' = 100$ kPa Used as Applied Loading for: (a) Irregular, (b) Regular Seismic Excitations

Table 2. Characteristic Parameters of Irregular and Regular Loadings

Parameters	Irregular	Regular
Loading pattern	Stress-controlled	Stress-controlled
Loading	Applied based on Bhuj (0.103 g), Tezpur (0.36 g) and Kobe (0.834 g)	Applied based on CSR = 0.05, 0.1, 0.2, 0.3
Confining stress σ_c' (kPa)	Applied based on confining depth of 2.5 m, 5.0 m and 7.5 m	50, 100, 200
Relative density D_r (%)	30, 60, 90	30, 60, 90
Frequency (Hz)	Overall shaking duration	1

The acceleration time histories of three strong motions (Bhuj, 2001, PGA = 0.103 g; Tezpur, 2012, scaled PGA = 0.36 g, and Kobe, 1995, PGA = 0.834 g) are chosen as the irregular seismic excitations, the characteristics of which in the time- and frequency-domain are presented in Fig. 3. The stress-time histories of the selected motions are evaluated as per the proposition of Seed and Idriss (1971), as detailed Kumar et al. (2018). Fig. 4(a) shows a typical plot of the irregular deviatoric stress-time histories for the aforementioned strong motions, which were applied on BS specimens prepared at $\sigma_c' = 100$ kPa (equivalent to a BS specimen collected from 5 m below the ground surface, considering a ground surface water table and saturated unit weight of BS is 20 kN/m^3).

For conducting laboratory experiments using regular excitations, the equivalent uniform shear stress cycles (τ_{cyc}) were estimated as 65% of the maximum shear stress (τ_{max}) of the irregular stress-time histories (as per Seed and Idriss, 1971). Based on PGA of irregular excitations, CSR ($= \tau_{cyc}/\sigma_c' = \sigma_d/2\,\sigma_c'$) for regular excitation

were obtained to be in the range of 0.05 – 0.75 (σ_d is the deviatoric stress). Accordingly, the average cyclic deviatoric stress for regular excitation was evaluated as 65% of the maximum deviatoric stress of the irregular motion, at a specific value of effective confining stress. Fig. 4(b) represents a typical regular deviatoric stress (σ_d) history applied on BS specimens. The investigating parameters of irregular and regular loadings are presented in Table 2.

Owing to a wide range of frequency present in a seismic motion, the selection of any particular frequency to be used in a regular excitation is a challenging task. For the strong motions chosen in the present study, the predominant and second-mode frequencies (associated with the maximum energy content of the strong motions) are found to be in the range of 0.5 – 4 Hz, which is within the global predominant frequency range of earthquakes i.e., 0.5 – 10 Hz (Bhattacharya, 2007). Based on the cyclic triaxial tests conducted using regular loading (f: 0.5 – 4 Hz), Kumar et al. (2015) reported that the excess PWP increases up to a frequency of 2 Hz and decreases thereafter, and the damping ratio (evaluated from first cycle) decreases beyond a frequency of 1 Hz. Several literatures have reported about the effect of frequency on the dynamic behaviour of soils (Kramer, 1996; Ishihara, 1996; Teachavorasinskun et al., 2002; Yilmaz et al., 2004; Ravishankar et al., 2005; Jakka et al., 2010; Maheshwari et al., 2012; Lombardi et al., 2014; Chattaraj and Sengupta, 2016, 2017). Based on the experimental investigations and the aforementioned literatures, the frequency of 1 Hz is chosen to represent the applied harmonic regular excitations for all the tests reported in this study.

4. Results and Discussions

4.1 Response of Brahmaputra Sand Specimens to Irregular Seismic Excitations

This section reports the behaviour of BS specimens under the chosen irregular excitations. The test results are presented in terms of the variation in shear strains and excess PWP ratio ($r_u = u_e/\sigma_c'$, u_e is the excess pore water pressure due to cyclic loading).

4.1.1 Influence of σ_c', D_r and γ_{max} on Initiation of Liquefaction

Figure 5 shows the results obtained for reconstituted BS specimens (D_r = 30%) subjected to different confining pressures (representative of different confining depths). Fig. 5(a) depicts the development of γ and r_u in BS specimen under the influence of Bhuj motion. γ_{max} was found to be nearly 0.01%, 0.03% and 0.03% at σ_c' = 50 kPa, 100 kPa and 150 kPa, respectively. As obvious, the specimens subjected to higher shear stress indicated a higher accumulation of shear strain. On the other hand, r_u was found to be very low ($r_{u,max}$ = 0.1 << 1), owing to the very low CSR values at different confining depths (0.097, 0.092 and 0.078 at 2.5, 5.0 and 7.5 m of depth, respectively, due to PGA = 0.103 g). Further, owing to the low PGA of Bhuj motion, it is observed that all the specimens, at different confining pressures, showed nearly similar value of γ_{max} and $r_{u,max}$.

Figures 5(b) illustrates the response of BS specimens at different σ_c' utilizing the scaled Tezpur motion. It is seen that γ_{max} varies in the range of 0.06 – 1.8%, against the variation of σ_c' in the range of 50 – 150 kPa. It is observed that at both σ_c' = 100 kPa and 150 kPa, the BS specimen shows initiation of liquefaction (r_u ≈ 1); whereas, no liquefaction was observed in the specimens

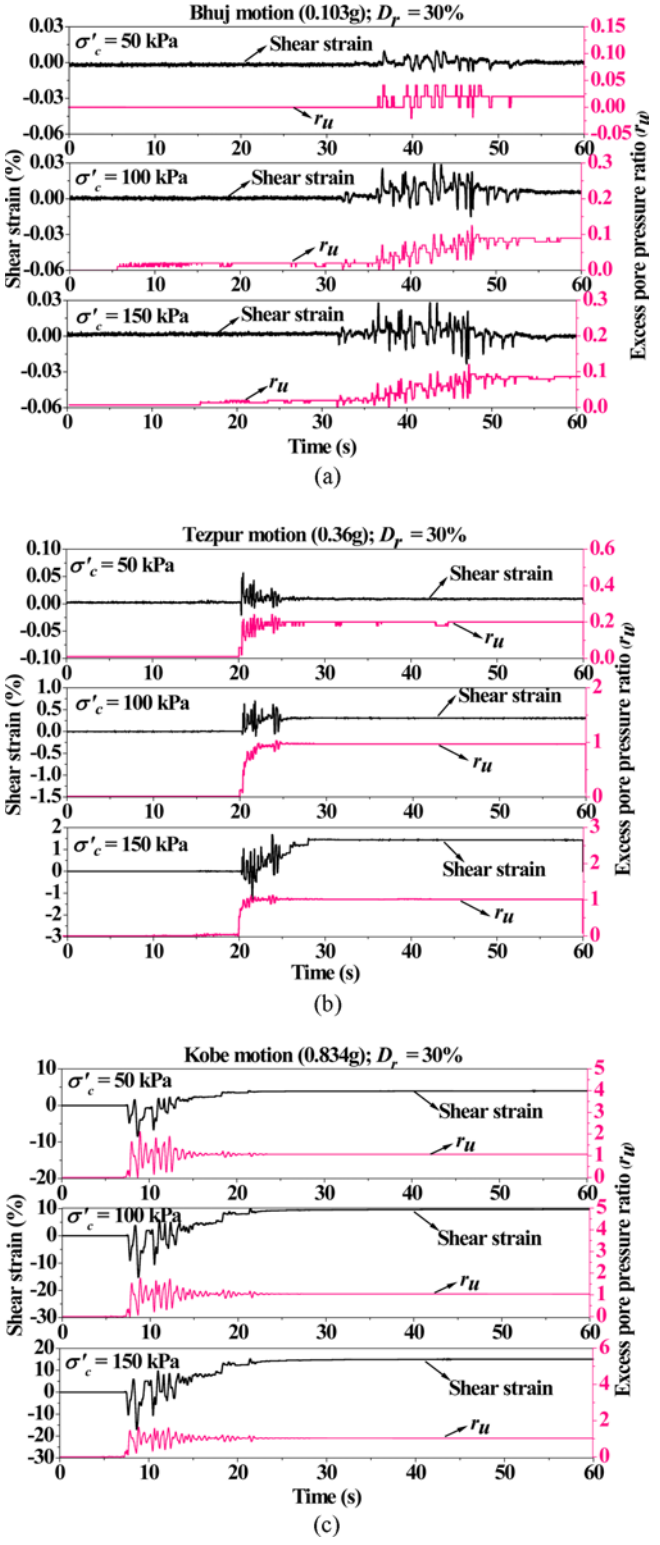

Fig. 5. Variation of γ and r_u in BS Specimens Prepared at D_r = 30% when Subjected to: (a) Bhuj, (b) Tezpur, (c) Kobe Motions

under the influence of σ_c' = 50 kPa, as highlighted by significantly lesser r_u ($r_{u,max}$ = 0.25 << 1). A significant amount of residual shear strain is observed when the BS specimen liquefies, indicating permanent deformation of soil. Similar permanent deformation in soil is also reported by researchers (Suetomi and Yoshida, 1998; Kumar et al., 2014a, 2014b). Fig. 5(c) presents the response of BS specimens utilizing Kobe motion. It is seen that at any confining pressure, BS specimens liquefied (as r_u reaches 1) and illustrated residual γ (> 5%).

Figure 6 illustrates the effective stress paths obtained from the irregular seismic loading of BS specimens constituted at D_r = 30%. These stress paths represents the state of stresses in the soil specimen during cyclic loading. Fig. 6(a) presents the response of BS specimen subjected to Bhuj motion of PGA = 0.103 g. It is found that the BS specimens (at the mentioned σ_c' = 50 kPa, 100 kPa and 150 kPa) do not show signs of liquefaction initiation since the mean effective stress does not reach zero. This is attributed to the development of very low magnitude of maximum shear strain (γ_{max} = 0.01%, 0.03% and 0.03% at σ_c' = 50 kPa, 100 kPa and 150 kPa, respectively). Fig. 6(b) shows that the Tezpur motion (PGA = 0.36 g) does not reflect initiation of liquefaction at σ_c' = 50 kPa whereas BS at σ_c' = 100 kPa and 150 kPa is found to liquefy as the mean effective stress becomes zero. This is attributed to the high value of γ_{max} (0.70% and 1.8% corresponding to σ_c' = 100 kPa and 150 kPa, respectively) developed in the specimen in comparison to γ_{max} = 0.06% corresponding to σ_c' = 50 kPa. Fig. 6(c) reveals that liquefaction is initiated at all the three BS specimens (σ_c' = 50 kPa, 100 kPa and 150 kPa) when they are subjected to Kobe motion of PGA = 0.834 g. This is due to the significantly higher values of $\gamma_{max} \geq$ 8% at all effective confining pressures. Therefore, it is evident that that with the increase of σ_c' and PGA of the strong motion, there is a noticeable increase in γ_{max}, thereby resulting in more prominent onset and manifestation of liquefaction. Hence, it can be summed up that along with effective confining stress and PGA of strong motion, the maximum shear strain plays a governing role as well in the initiation of liquefaction in a

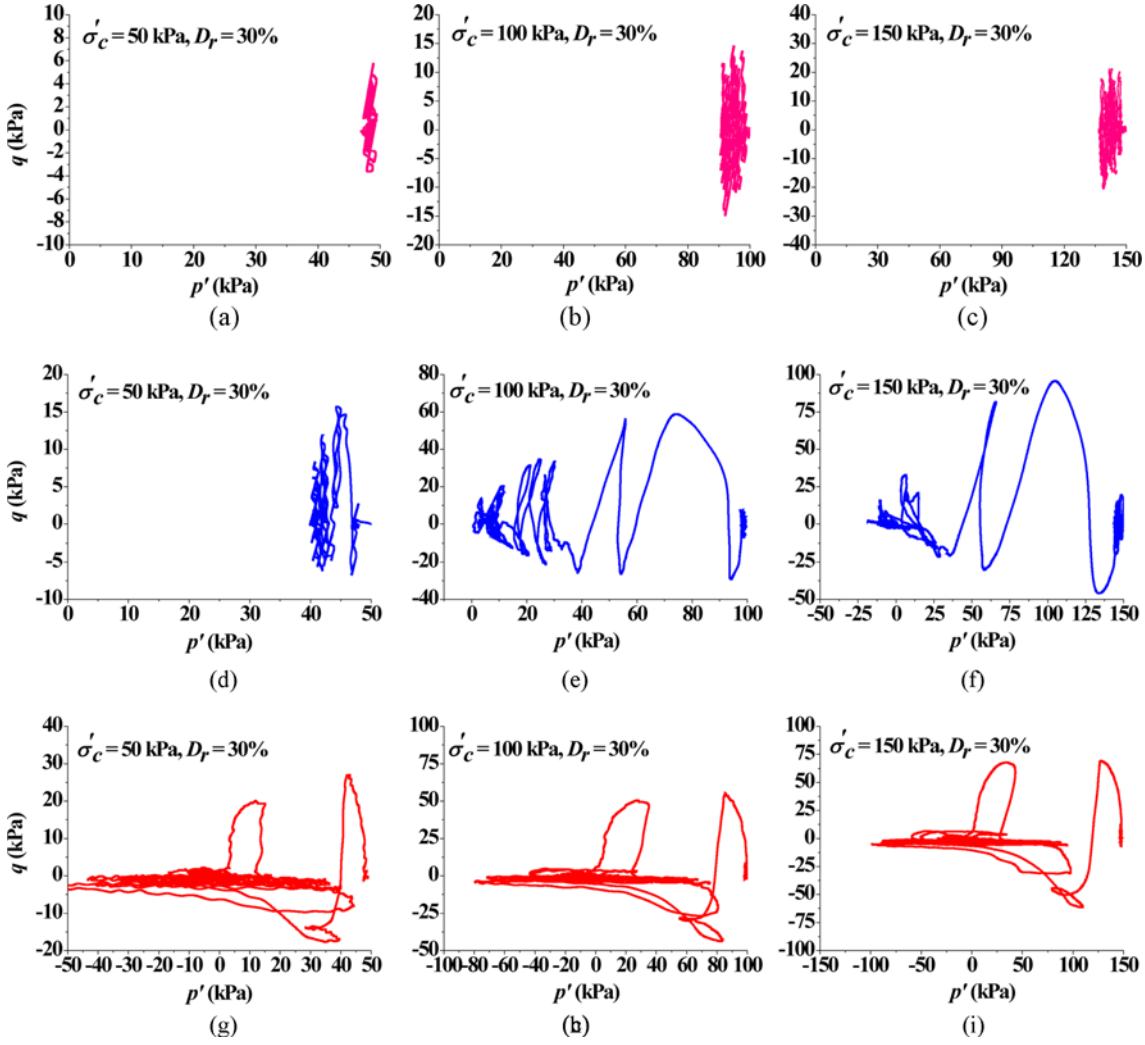

Fig. 6. Effective Stress Paths Obtained During Irregular Excitation of BS Specimens at Different σ_c' and D_r = 30%: (a) Bhuj Motion (σ_c' = 50 kPa, D_r = 30%), (b) Bhuj Motion (σ_c' = 100 kPa, D_r = 30%), (c) Bhuj Motion (σ_c' = 150 kPa, D_r = 30%), (d) Tezpur Motion (σ_c' = 50 kPa, D_r = 30%), (e) Tezpur Motion (σ_c' = 100 kPa, D_r = 30%), (f) Tezpur Motion (σ_c' = 150 kPa, D_r = 30%), (g) Kobe Motion (σ_c' = 50 kPa, D_r = 30%), (h) Kobe Motion (σ_c' = 100 kPa, D_r = 30%), (i) Kobe Motion (σ_c' = 150 kPa, D_r = 30%)

Table 3. Summary of Investigations on BS Specimen Subjected to Different σ_c'

Input motion	σ_c' (kPa)	D_r (%)	CSR_{max}	γ_{max} (%)	τ_{max} (kPa)	G (MPa) = τ_{max}/γ_{max}	$r_{u,max}$	$r_{u,residual}$	Liquefaction
Bhuj (0.103 g)	50	30	0.097	0.01	4.85	48.50	0.05	0.025	No
	100		0.092	0.03	9.2	30.67	0.13	0.09	
	150		0.078	0.03	11.7	39.00	0.13	0.09	
Tezpur (0.36 g)	50	30	0.346	0.06	17.3	28.84	0.25	0.24	No
	100		0.327	0.70	32.7	4.67	1.00	0.90	Yes
	150		0.278	1.80	41.7	2.32	1.20	1.00	
Kobe (0.834 g)	50	30	0.802	8.00	40.1	0.50	2.25	1.00	Yes
	100		0.756	15.0	75.6	0.50	1.75	1.00	
	150		0.645	18.0	96.7	0.54	1.75	1.00	

Table 4. Summary of Investigations on BS Specimens Prepared at Different D_r

Input motion	D_r (%)	σ_c' (kPa)	CSR_{max}	γ_{max} (%)	τ_{max} (kPa)	G (MPa)	$r_{u,max}$	$r_{u,residual}$	Liquefaction
Bhuj (0.103 g)	30	100	0.092	0.03		30.67	0.13	0.09	No
	60			0.03	9.2	30.67	0.09	0.05	
	90			0.02		46.00	0.08	0.03	
Tezpur (0.36 g)	30	100	0.327	0.70		4.66	1.0	0.9	Yes
	60			0.52	32.7	6.27	1.0	1.0	
	90			0.50		6.52	0.9	0.9	
Kobe (0.834 g)	30	100	0.756	15.0		0.50	2.0	1.00	Yes
	60			12.0	75.6	0.63	1.7	1.00	
	90			5.00		1.51	1.5	1.00	

cohesionless soil. The increase in γ_{max} is primarily governed by the increase in the deviatoric stress with the increase in the confining stress, thereby soils at higher confining stress exhibit initiation of liquefaction.

Tables 3 and 4 summarizes the response of BS specimens subjected to irregular excitations. Table 3 shows that for any of the strong motion, γ_{max} increases with the increase in σ_c'. In the saturated BS specimens, r_u increases with the increase of γ_{max}, resulting in substantial reduction in shear stiffness (G). This is mainly due to the substantial increase in deviatoric stress (σ_d) and shear strains (γ) along with the increase in σ_c'. Table 4 shows that for each of the strong motions, γ_{max} decreases with the increase in D_r; at the same time, a reduction in r_u is observed, indicating reduction of liquefaction potential. In a nutshell, it can be summarized that although the individual increase of σ_c' and D_r on the change in liquefaction potential is in contrary to each other, the onset of liquefaction is primarily controlled by γ_{max}, and the onset is inevitable when γ exceeds 0.5%.

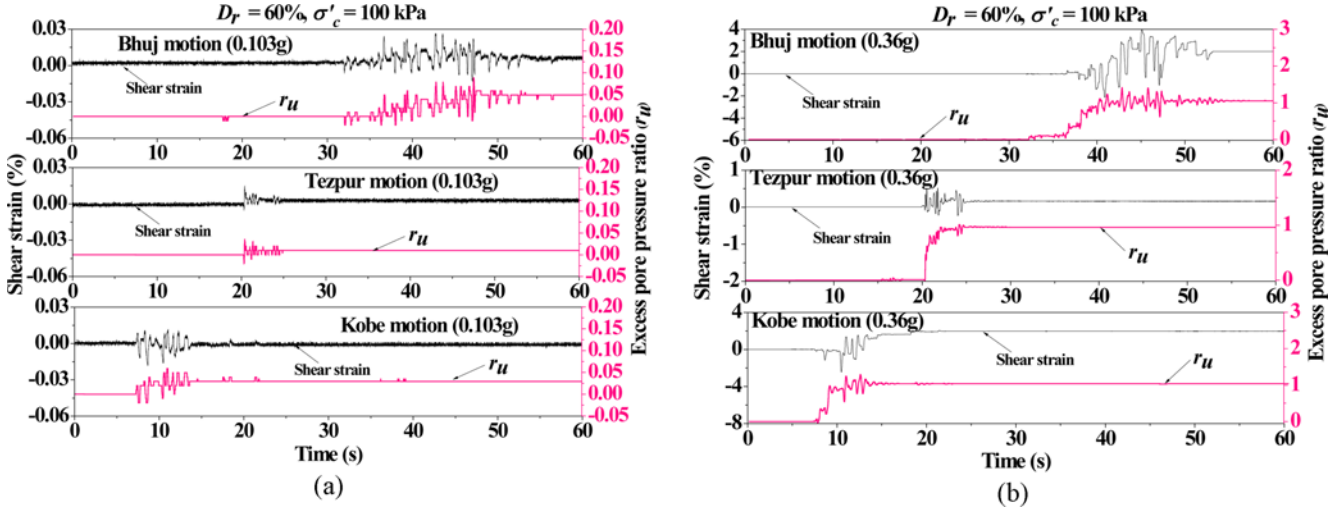

Fig. 7. Observed Strain Accumulation and Excess PWP Ratio in the BS Specimens (D_r = 60% and σ_c' = 100 kPa) Subjected to Scaled Strong Motions: (a) PGA = 0.103 g, (b) PGA = 0.36 g

Table 5. Summary of Investigations on BS Specimens Subjected to Ground Motions Scaled to the Same Magnitude of PGA

Input motion	Scaled PGA(g)	D_r (%)	σ_c' (kPa)	CSR_{max}	τ_{max} (kPa)	γ_{max} (%)	G (MPa)	$r_{u,residual}$	Lique-faction
Bhuj	0.103	60	100	0.092	9.2	0.026	35.38	0.05	No
Tezpur						0.015	62.00	0.01	
Kobe						0.019	48.42	0.025	
Bhuj	0.36	60	100	0.327	32.7	4.00	0.81	1.00	Yes
Tezpur						0.52	6.29	1.00	
Kobe						2.50	1.30	1.00	

Table 6. Ground Motion Parameters of Scaled Motions with PGA of 0.103 g and 0.36 g

Parameters	Bhuj	Tezpur	Kobe	Bhuj	Tezpur	Kobe
	(0.103 g)			(0.36 g)		
Predominant period (s)	0.26	0.14	0.36	0.26	0.14	0.36
Mean period (s)	0.59	0.23	0.64	0.59	0.23	0.64
Bracketed duration (s)	55.18	30.72	21.92	55.18	30.72	21.92
Significant duration (s)	14.84	9.04	8.38	14.84	9.04	8.38
Arias intensity (m/sec)	0.268	0.074	0.14	3.12	0.9	1.73
Specific energy density (cm^2/sec)	438.561	8.7	128.57	5351	106.6	1570.4
v_{max}/a_{max} (sec)	0.13	0.03	0.10	0.13	0.03	0.10

4.1.2 Effect of Strong Motion Parameters on the Soil Liquefaction

To establish the influence of strong motion parameters on the liquefaction of BS specimens, all the three chosen strong motions were linearly amplitude-scaled to a specific PGA = 0.103 g and 0.36 g. Fig. 7 illustrates the responses of BS specimen, prepared at D_r = 60% and σ_c' = 100 kPa. Fig. 7(a) shows that when scaled to PGA = 0.103 g, none of the strong motions could initiate the liquefaction in BS specimens. Subjected to the same input PGA, the specimens exhibit different γ_{max}, in the order Bhuj (0.103 g) > Kobe (0.103 g) > Tezpur (0.103 g), as shown in Table 5. This is attributed to the Arias intensity and specific energy density of the strong motion, which exhibits a similar decreasing trend, as shown in Table 6. Fig. 7(b) presents the behaviour of BS specimens subjected to scaled PGA of 0.36 g. Table 5 shows that the trend of variation in γ_{max} under the influence of PGA = 0.36 g is similar as obtained for the former scenario. All of BS specimens exhibit liquefaction when subjected to scaled motions of PGA = 0.36 g, due to substantially higher values of Arias intensity and specific energy density in comparison to the former scenario. Overall, it can be stated that the responses are largely influenced by the energy content of the strong motion. The onset of soil liquefaction is also influenced by the waveforms and durations of earthquakes (Sassa and Yamazaki, 2017), which is beyond the scope of this paper.

4.1.3 Dynamic Response of Brahmaputra Sand from Cyclic Triaxial Tests Using Irregular Excitations

Figure 8 illustrates the overall variation of G and r_u with shear strain in BS specimens (prepared at different combinations of σ_c' and D_r) when subjected to different irregular excitations. The

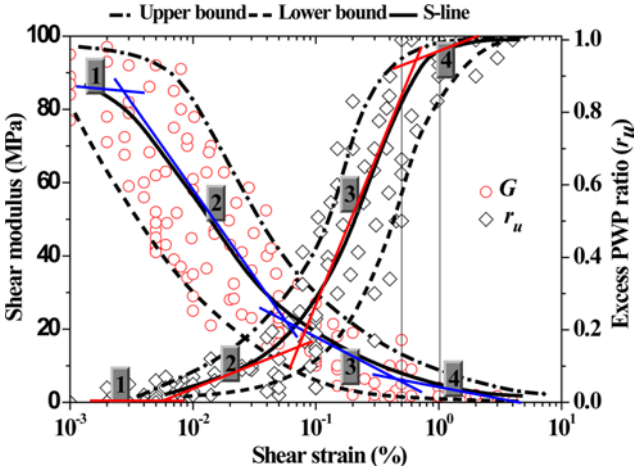

Fig. 8. Variation of G and r_u with γ for BS Specimens Subjected to Irregular Excitations

variations of G and r_u are represented with the lower and upper bounds. Based on Seed and Idriss (1971) approach, the corresponding S-lines, representing the 65% of maximum values of G and r_u, are drawn. The tangent lines, plotted on the S-lines for G and r_u, reveal the variations of soil stiffness and excess PWP ratio with shear strains, and reveals an indicative range of shear strain at which BS is most likely to liquefy. Tangent Line-1 shows that at shear strain less than 0.01%, BS exhibits stiffest response (G_{max}) with minimal r_u (< 0.05), thereby indicating that the soil will not definitely liquefy. When the accumulated shear strain is in the range 0.01 – 0.1%, as represented by Tangent Line-2, r_u increases up to 0.2 and G decreases approximately to one-third of G_{max}. However, as indicated by experimental results,

liquefaction was not observed in this range of shear strain as well. In the shear strain range 0.1% – 0.5% (Tangent Line-3), the initiation of liquefaction is imminent, as r_u shows a significant increase to 0.8, along with a significant strength reduction, nearly to one-tenth of G_{max}. Once the shear strain increases beyond 0.5%, the BS specimens exhibit the onset of liquefaction while passing through a quasi-liquefaction zone (represented by Tangent Line-4). Overall, it can be stated that the strain-dependent behaviour of cohesionless soils, subjected to irregular seismic excitations, exhibits four distinct states before being fully liquefied, namely (a) no liquefaction (b) quasi-liquefaction (c) onset or initiation of liquefaction, and (d) complete liquefaction. For BS specimens, the zone of no liquefaction is prevalent in shear strains less than 0.5%, wherein G is greater than 10 MPa and r_u is less than 0.8. The quasi-liquefaction state is a specific condition in saturated soils subjected to dynamic loading, where the soil exhibits elevated excess PWP but yet to attain onset of liquefaction (Kiku and Yoshida, 2000). For BS specimens, the quasi-liquefaction zone is found to be within shear strains 0.5 – 0.75%, where G and r_u are in the ranges 5 – 10 MPa and 0.8 – 0.85, respectively. Once the quasi-liquefaction phase is reached, the onset of liquefaction in cohesionless soil can occur very quickly. Yoshida et al. (2008) reported that the onset of liquefaction arises when r_u is in the range of 0.85 – 1.0. In this study, the onset of liquefaction for BS is observed in a shear strain range of 0.75 –1%, manifested by a significantly reduced G (1 – 5 MPa) and a high r_u (in the range of 0.85 – 1.0). Complete liquefaction of BS is observed at shear strains greater than 1%, where $G < 1$ MPa and $r_u \geq 1$ is observed.

4.2 Response of Brahmaputra Sand Specimens to Regular Seismic Excitations

During an earthquake, neither the applied stress nor the applied strain remains constant. To identify the influence of both the variations, it is important to identify the effects in terms of both strain-controlled and stress controlled approaches. The strain controlled approaches are mostly chosen to identify the dynamic properties of soils, while the stress-controlled approached provides the idea of its liquefaction potential. In this study, for establishing the liquefaction potential of BS in terms of the accumulation of excess PWP and shear strains based on the number of load repetitions (N), stress-controlled CT tests were conducted using regular stress cycles. In stress-controlled CT tests, CSR is an index for the evaluation of cyclic strength of soils (ASTM D5311, 2013) which quantifies the applied stress in terms of the field confining stresses.

4.2.1 Variation of r_u and γ with Confining Depth

Figure 9 presents the response of BS specimens (D_r = 30%) subjected to σ_c' = 50, 100 and 200 kPa, representative of increasing confining depths. Fig. 9 highlights the accumulation of r_u of γ with increasing N. BS specimens were subjected to varying CSR, in the range of 0.05 – 0.3. Fig. 9(a) shows that when cyclically sheared to CSR = 0.2, BS specimens exhibit onset of liquefaction at N = 10, 4 and 3 cycles for σ_c' = 50 kPa, 100 kPa and 200 kPa,

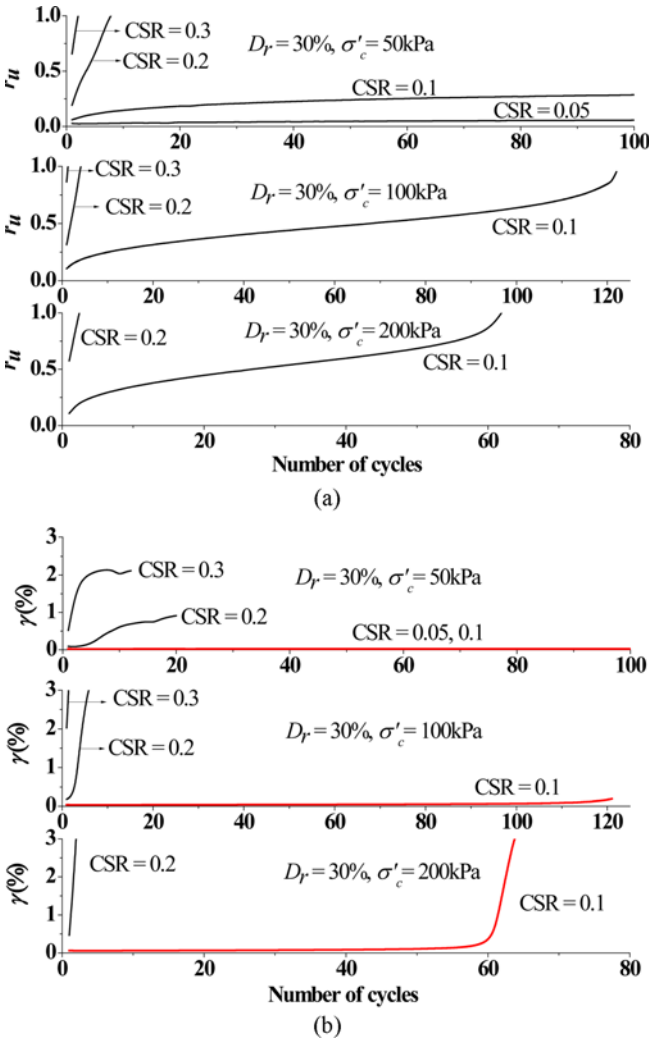

Fig. 9. Variation of: (a) r_u, (b) γ in BS Specimens Prepared at D_r = 30% and Subjected to Different σ_c' and CSR

respectively. For specimens subjected to CSR = 0.3, the onset is observed at N = 2 and 1.5 for σ_c' = 50 and 100 kPa, respectively. It is also observed that even at 500th cycle, BS specimens, at σ_c' = 50 kPa, did not liquefy when subjected to CSR = 0.05 and 0.1; whereas, when subjected to CSR = 0.1, BS specimens at σ_c' = 100 kPa and 200 kPa showed the onset at 122nd and 62nd cycles, respectively. Fig. 9(b) illustrates the shear strain accumulation in the BS specimens during cyclic shearing at different CSR values (0.05 – 0.3). For CSR = 0.2, accumulated γ at the onset of liquefaction is 0.5%, 2% and 3% at σ_c' = 50 kPa, 100 kPa and 200 kPa, respectively; whereas, for CSR = 0.3, the accumulated γ is greater than 1% for σ_c' = 50 kPa and 100 kPa. As earlier, for BS specimens at σ_c' = 50 kPa, $\gamma \approx 0.02\%$ till 500 cycles (Fig. 9(b)), thus onset of liquefaction is not observed at CSR = 0.05 and 0.1. At CSR = 0.1, the accumulated strain is observed to be 0.5% and 1.5%, when pronounced liquefaction is observed at N = 122nd and 62nd cycles for σ_c' = 100 kPa and 200 kPa, respectively (complying with Fig. 9(a)).

Thus, the overall observation indicates that for the same CSR,

Table 7. Summary of Response of BS Specimens Subjected to Regular Excitation

D_r (%)	σ_c' (kPa)	CSR	$G_{(1^{st}, cycle)}$ (MPa)	$\gamma_{(1^{st} cycle)}$ (%)	$r_{u,(1^{st} cycle)}$	N_L	G_{ru} (MPa)	γ_{ru} (%)	$r_{u,residual}$
30	50	0.05, 0.1, 0.2, 0.3	24, 22, 10, 2.5	0.01, 0.02, 0.09, 0.5	0.03, 0.06, 0.19, 0.65	NL*, NL, 8, 2	--, --, 1.2, 0.70	--, --, 0.45, 1.4	--, --, 1.02, 1.02
	100	0.1, 0.2, 0.3	23, 10, 1.2	0.04, 0.18, 2.0	0.10, 0.30, 0.85	125, 4, 1	1.5, 0.50, 0.45	0.5, 2.5, 4.5	1.00, 1.18, 1.35
	200	0.1, 0.2	33, 8	0.07, 0.47	0.10, 0.58	62, 3	0.90, 0.45	1.5, 6.8	1.00, 1.16
30	50	0.05, 0.1, 0.2, 0.3	24, 22, 10, 2.5	0.01, 0.02, 0.09, 0.5	0.03, 0.06, 0.19, 0.65	NL, NL, 8, 2	--, --, 1.2, 0.70	--, --, 0.45, 1.4	--, --, 1.02, 1.02
60	100	0.1, 0.2, 0.3	53, 27, 14	0.02, 0.14, 0.70	0.07, 0.27, 0.60	NL, 10, 3	--, 0.45, 0.50	--, 1.3, 3.5	--, 1.07, 1.2
90	200	0.1, 0.2, 0.3	56, 32, 13	0.04, 0.13, 0.48	0.10, 0.24, 0.45	NL, 12, 5	--, 1.5, 2.0	--, 2.0, 2.3	--, 1.05, 1.04

Note: N_L = Number of cycles to liquefaction, *NL = No liquefaction till 500 cycles; $G_{(1st, cycle)}$ = Shear modulus at first cycle; G_{ru} = Shear modulus at r_u = 1; γ_{ru} = Shear strain at r_u = 1

an increase in confining depth results in the reduction of the number of cycles required to initiate liquefaction of BS specimen. This is attributed to the fact that for same CSR, increase in σ_c' results in substantial increase in σ_d and associated shear strains, thereby reducing the number of cycles required for the onset of liquefaction (as summarized in Table 7). This is stated as the stress dependency of liquefaction as reported by the researchers based on similar observations (Simatupang and Okamura, 2017; Wang et al., 2017). This finding can apparently lead to the impression that soil strata at larger depths will undergo quicker initiation of liquefaction. However, the incidences of soil liquefaction, as observed in several past earthquakes, is mostly restricted to a shallow depth phenomenon within 15 m from the ground surface (Seed and Idriss, 1971; Elgamal et al., 1996; Byrne et al., 2004; Sreng et al., 2015; Qu et al., 2016). During an earthquake occurrence, the same deviatoric stress is applied on the entire stratified soil. Thus, as the confining pressure is higher at successive deeper stratum, the CSR attains a progressive lesser magnitude with depth, and thereby successive deeper layers require more number of stress cycles to liquefy. Hence, in this context, the current findings from a stress-controlled cyclic triaxial test is no different from the field observations. In the stress controlled CT tests, the same CSR is maintained while the applied deviator stress is increased, thus resulting in an apparent misrepresentation of the finding. Therefore, in the light of the above discussion, a judicious approach should be exercised in understanding and representing the dynamic response of soils to earthquakes, owing to the fact that none of the entities (relative density, confining stress, CSR, and deviatoric stress) remains constant in practice, as opposed to the conduct of laboratory investigations.

4.2.2 Variation of r_u and γ with Simultaneous Increase of σ_c' and D_r

Table 7 lists the response of BS specimens subjected to regular excitations at various testing conditions (relative density, confining stress and CSR). The results are presented in terms of G, γ and r_u, calculated after first loading cycle and at the state of liquefaction. It is observed that for CSR = 0.2 and 0.3, the specimens prepared at D_r = 30% and σ_c' = 50 kPa requires lesser number of stress cycles to attain liquefaction (8 cycles), in comparison to the specimens prepared at D_r = 60%, σ_c' = 100 kPa (10 cycles) and D_r = 90%, σ_c' = 200 kPa (12 cycles). Section 4.2.1 elucidated that the liquefaction potential of BS specimens decrease with the increase in D_r, while the same increases with the increase in σ_c'. It is observed when subjected to CSR = 0.05 and 0.1, BS specimens, prepared at any D_r and σ_c', do not exhibit liquefaction even until a very large numbers of loading cycles. On the other hand, specimens subjected to higher CSR (0.2 or 0.3) manifested the occurrence of liquefaction. BS specimens at D_r = 30% and σ_c' = 50 kPa show initiation of liquefaction at the 8th and 2nd cycle for CSR = 0.2 and 0.3, respectively. Similarly, BS specimens at D_r = 60% and σ_c' = 100 kPa exhibit liquefaction at the 10th and 3rd cycles for CSR = 0.2 and 0.3, whereas, liquefaction is observed at the 12th and 5th cycles in specimens prepared at D_r = 90% and σ_c' = 200 kPa for the stated magnitudes of CSR.

Table 7 also shows that the specimens at D_r = 30% and σ_c' = 50 kPa exhibit substantially low magnitudes of shear strain ($\gamma \leq$ 0.2%) at CSR = 0.05 and 0.1. It can be noticed that with the simultaneous increase in the D_r (30%, 60% and 90%) and σ_c' (50, 100 and 200 kPa, respectively), BS portrays the onset of liquefaction at CSR = 0.2 in the 8th, 10th and 12th cycles, respectively. In each case, the corresponding γ has reached or exceeded 0.5%. BS specimens, at varying combinations of D_r and σ_c', when subjected to CSR = 0.3, portray the initiation of

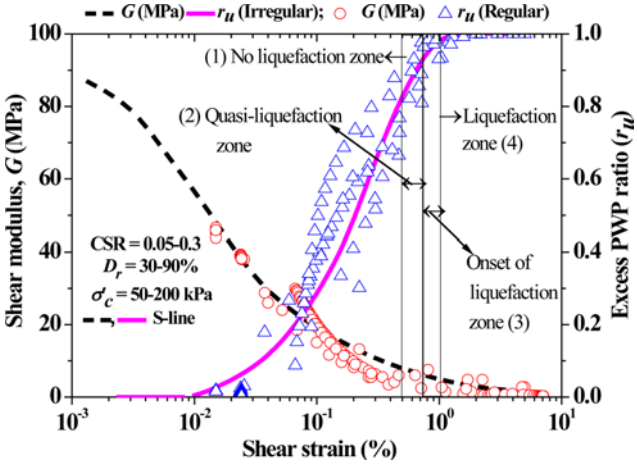

Fig. 10. Comparison of the Strain-Dependent G and r_u in BS Specimens Based on Stress-Controlled Cyclic Triaxial Test Using Irregular and Regular Excitations

liquefaction at N = 2, 3 and 5 cycles, respectively, and in each case, γ is observed to be greater than 0.5%.

4.2.3 Dynamic Response of Brahmaputra Sand Specimens from Cyclic Triaxial Tests Using Regular Excitations

Similar to that observed for irregular excitation, the entire variation of strain-dependent r_u and G, as obtained from regular excitations, can be categorised into the previously stated four zones. Fig. 10 depicts the comparative strain-dependent variations of G and r_u of BS specimens obtained from irregular and regular excitations, which exhibits an appreciable agreement. The zone of no liquefaction in demarcated with $\gamma < 0.5\%$, $G > 10$ MPa and $r_u < 0.8$. The quasi-liquefaction zone is spread over γ in the range 0.5 – 0.75%, G in the range 5 – 10 MPa and r_u in the range 0.8 – 0.9. The onset of liquefaction is represented by γ in the range 0.75 – 1%, G in the range 1 – 5 MPa and r_u in the range 0.9 – 1.0. The liquefaction zone is observed at $\gamma > 1\%$, with $G < 1$ MPa and $r_u \geq 1$. These observations suggest that both regular and irregular excitations can be equally used for the assessment of liquefaction potential of cohesionless soils. The present study on Brahmaputra sand clearly identified $\gamma = 1\%$ as the limiting criterion for the onset of liquefaction, apart from the general criterion of r_u reaching or exceeding the value of 1.

5. Conclusions

This paper describes the dynamic response of Brahmaputra sand subjected to regular and irregular excitations using stress-controlled cyclic triaxial testing. The conclusions are drawn from this study are as follows:

1. With increase in relative density, BS exhibits a decrease in the liquefaction potential, while the latter increases with increasing CSR.
2. The liquefaction characteristics of cohesionless soil can be equally assessed by stress-controlled cyclic triaxial tests using regular or irregular excitations.
3. For saturated sandy soils, the strain-dependent shear modulus and excess PWP ratio is categorized into four zones, namely the zone of no liquefaction, quasi-liquefaction zone, onset of liquefaction and fully liquefied condition.
4. Brahmaputra sand do not exhibit liquefaction up to γ = 0.5%. The quasi liquefaction state is observed in the range 0.5 – 0.75%, while the onset of liquefaction culminates in the range 0.75 – 1%.
5. $\gamma \geq 0.5\%$ (for regular and irregular excitation), PGA ≥ 0.36 g (for irregular excitation) and CSR > 0.3 (for regular excitation) are adjudged as the limiting criteria for the quasi-liquefaction and subsequent onset of liquefaction in Brahmaputra sand.

Acknowledgements

Not Applicable

ORCID

Arindam Dey https://orcid.org/0000-0001-7007-2729
A Murali Krishna https://orcid.org/0000-0002-5422-2501

References

ASTM D854 (2014) Standard test methods for specific gravity of soil solids by water pycnometer. ASTM D854, ASTM International, West Conshohocken, PA, USA, DOI: 10.1520/D0854-14

ASTM D2487 (2011) Standard practice for classification of soils for engineering purposes (unified soil classification system). ASTM D2487, ASTM International, West Conshohocken, PA, USA, DOI: 10.1520/D2487-11

ASTM D4253 (2016) Standard test methods for maximum index density and unit weight of soils using a vibratory table. ASTM D4253, ASTM International, West Conshohocken, PA, USA, DOI: 10.1520/D4253-16

ASTM D4254 (2016) Standard test methods for minimum index density and unit weight of soils and calculation of relative density. ASTM D4254, ASTM International, West Conshohocken, PA, USA, DOI: 10.1520/D4254-16

ASTM D5311/D5311M (2013) Standard test method for load controlled cyclic triaxial strength of soil. ASTM D5311/D5311M, ASTM International, West Conshohocken, PA, USA, DOI: 10.1520/D5311_D5311M

ASTM D7928 (2017) Standard test method for particle-size distribution (gradation) of fine-grained soils using the sedimentation (hydrometer) analysis. ASTM D7928, ASTM International, West Conshohocken, PA, USA, DOI: 10.1520/D7928-17

Basu D, Dey A, Kumar SS (2017) One-dimensional effective stress non-Masing nonlinear ground response analysis of IIT Guwahati. *International Journal of Geotechnical Earthquake Engineering* 8(1):1-27, DOI: 10.4018/IJGEE.2017010101

Bhattacharya S (2007) Design of foundations in seismic areas: Principles and applications. National Information Centre of Earthquake Engineering, Indian Institute of Technology Kanpur, Kanpur, India, 477

Byrne PM, Park SS, Beaty M, Sharp M, Gonzalez L, Abdoun T (2004) Numerical modeling of liquefaction and comparison with centrifuge tests. *Candian Geotechnical Journal* 41:193-211, DOI: 10.1139/t03-088

Chattaraj R, Sengupta A (2016) Dynamic properties of fly ash. *Journal of Material in Civil Engineering*, DOI: 10.1061/(ASCE)MT.1943-5533.0001712

Chattaraj R, Sengupta A (2017) Liquefaction potential and strain dependent dynamic properties of Kasai river sand. *Soil Dynamics and Earthquake Engineering* 90:467-475, DOI: 10.1016/j.soildyn.2016.07.023

Chung RM, Yokel FY, Drnevich VP (1984) Evaluation of dynamic properties of sands by resonant column testing. *Geotechnical Testing Journal* 7:60-69, DOI: 10.1520/GTJ10594J

Dobry R, Abdoun T (2015) Cyclic shear strain needed for liquefaction triggering and assessment of overburden pressure factor K_σ. *Journal of Geotechnical and Geoenvironmental Engineering* 141:04015047, DOI: 10.1061/(ASCE)GT.1943-5606.0001342

Dobry R, Abdoun T, Stokoe KH, Moss RES, Hatton M, El Ganainy H (2015) Liquefaction potential of recent fills versus natural sands located in high-seismicity regions using shear-wave velocity. *Journal of Geotechnical and Geoenvironmental Engineering* 141:04014112-1-

13, DOI: 10.1061/(ASCE)GT.1943-5606.0001239
Dobry R, Ladd RS, Yokell FY, Chung RM, Powell D (1982) Prediction of pore water pressure buildup and liquefaction of sands during earthquakes by the cyclic strain method. US Department of Commerce, National Bureau of Standards, Gaithersburg, MD, USA, 138
Elgamal AW, Zeghal M, Taboada V, Dobry R (1996) Analysis of site liquefaction and lateral spreading using centrifuge testing records. *Soils and Foundations* 36:111-121, DOI: 10.3208/sandf.36.2_111
Head KH (1992) Manual of soil laboratory testing, vol. 3, effective stress tests. John Willy & Sons, New York, NY, USA
Hardin BO, Drnevich VP (1972) Shear modulus and damping in soils: Measurement and parameters effects. *Journal of Soil Mechanics and Foundations Division* 98:603-624
Hsu CC, Vucetic M (2004) Volumetric threshold shear strain for cyclic settlement. *Journal of Geotechnical and Geoenvironmental Engineering* 130:58-70, DOI: 10.1061/(ASCE)1090-0241(2004)130:1(58)
IS-1893 (2002) Criteria for earthquake resistant design of structures-general provisions and buildings. IS-1893, Bureau of Indian Standard, New Delhi, India
Ishibashi, I, Zhang, X (1993) Unified dynamic shear moduli and damping ratios of sand and clay. *Soils and Foundations* 33:182-191, DOI: 10.3208/sandf1972.33.182
Ishihara K (1996) Soil behaviour in earthquake geotechnics. Oxford science publications, Oxford, UK
Ishihara K, Troncoso J, Kawase Y, Takahashi Y (1980) Cyclic strength characteristics of tailings materials. *Soils and Foundations* 20:127-142, DOI: 10.3208/sandf1972.20.4_127
Ishihara K, Yasuda S (1972) Soil liquefaction due to irregular excitation. *Soils and Foundations* 12:65-77, DOI: 10.3208/sandf1972.12.4_65
Ishihara K, Yasuda S (1975) Sand liquefaction in hollow cylinder torsion under irregular excitation. *Soils and Foundations* 15:45-59, DOI: 10.3208/sandf1972.15.45
Iwasaki T, Tatsuoka F, Takagi Y (1978) Shear modulus of sands under cyclic torsional shear loading. *Soils and Foundations* 18(1):39-56, DOI: 10.3208/sandf1972.18.39
Jakka RS, Datta M, Ramana GV (2010) Liquefaction behaviour of loose and compacted pond ash. *Soil Dynamics and Earthquake Engineering* 30:580-590, DOI: 10.1016/j.soildyn.2010.01.015
Kiku H, Yoshida, N (2000) Dynamic deformation property tests at large strains. 12th world conference on earthquake engineering, January 30-February 4, Auckland, New Zealand
Kokusho T, Yoshida Y, Esashi Y (1982) Dynamic properties of soft clay for wide strain range. *Soils and Foundations* 22:1-18, DOI: 10.3208/sandf1972.22.4_1
Kramer SL (1996) Geotechnical earthquake engineering. Prentice Hall, Upper Saddle River, NJ, USA
Kumar SS, Dey A, Krishna AM (2014a) Equivalent linear and nonlinear ground response analysis of two typical sites at Guwahati city. Proceedings of Indian geotechnical conference, December 18-20, Kakinada, India
Kumar SS, Dey A, Krishna AM (2015) Dynamic response of river bed sands using cyclic triaxial tests. 5th young Indian geotechnical engineers conference, March 14-15, Vadodara, India
Kumar SS, Krishna AM, Dey A (2014b) Nonlinear site-specific ground response analysis: Case study of Amingaon, Guwahati. 15th symposium on earthquake engineering, December 11-13, IIT Roorke, India
Kumar SS, Krishna AM, Dey A (2017) Evaluation of dynamic properties of sandy soil at high cyclic strains. *Soil Dynamics and Earthquake Engineering* 99:157-167, DOI: 10.1016/j.soildyn.2017.05.016
Kumar SS, Krishna AM, Dey A (2018) Response of saturated cohesionless soil subjected to seismic excitations. *Natural Hazards* 93(1):509-529, DOI: 10.1007/s11069-018-3312-1
Ladd RS, Dobry R, Dutko P, Yokel FY, Chung RM (1989) Pore-water pressure build-up in clean sands because of cyclic straining. *Geotechnical Testing Journal* 12:77-86, DOI: 10.1520/GTJ10677J
Lombardi D, Bhattacharya S, Hyodo M, Kaneko T (2014) Undrained behaviour of two silica sands and practical implications for modelling SSI in liquefiable soils. *Soil Dynamics and Earthquake Engineering* 66:293-304, DOI: 10.1016/j.soildyn.2014.07.010
Maheshwari BK, Kale SS, Kaynia AM (2012) Dynamic properties of Solani sand at large strains: A parametric study. *International Journal of Geotechnical Engineering* 6:353-358, DOI: 10.3328/IJGE.2012.06.03.353-358
Nath SK, Thingbaijam KKS, Raj A (2008) Earthquake hazard in Northeast India – A seismic microzonation approach with typical case studies from Sikkim Himalaya and Guwahati city. *Journal of Earth System and Science* 117:809-831, DOI: 10.1007/s12040-008-0070-6
Qu M, Xie Q, Cao X, Zhao W, He J, Jin J (2016) Model test of stone columns as liquefaction countermeasure in sandy soils. *Frontier of Structural and Civil Engineering* 10:481-487, DOI: 10.1007/s11709-016-0355-9
Raghukanth STG, Dash SK (2010) Evaluation of seismic soil-liquefaction at Guwahati city. *Environmental Earth Science* 61:355-368, DOI: 10.1007/s12665-009-0347-3
Raghukanth STG, Sreelatha S, Dash SK (2008) Ground motion estimation at Guwahati city for an M_w 8.1 earthquake in the Shillong plateau. *Tectonophysics* 448:98-114, DOI: 10.1016/j.tecto.2007.11.028
Ravishankar BV, Sitharam TG, Govindaraju L (2005) Dynamic properties of Ahmedabad sands at large strains. Proceedings of Indian geotechnical conference, December 17-18, Ahmedabad, India, 369-372
Sassa S, Yamazaki H (2017) Simplified liquefaction prediction and assessment method considering waveforms and durations of earthquakes. *Journal of Geotechnical and Geoenvironmental Engineering* 143:04016091-1-13, DOI: 10.1061/(ASCE)GT.1943-5606. 0001597
Sawada S, Tsukamoto Y, Ishihara K (2006) Residual deformation characteristics of partially saturated sandy soils subjected to seismic excitation. *Soil Dynamics and Earthquake Engineering* 26:175-182, DOI: 10.1016/j.soildyn.2004.11.024
Seed HB, Idriss IM (1971) Simplified procedure for evaluating soil liquefaction potential. *Journal of Soil Mechanics and Foundation Division* 97:1249-1273
Seed HB, Lee KL (1966) Liquefaction of saturated sands during cyclic loading. *Journal of Soil Mechanics and Foundation Division* 92:105-134
Seed HB, Wong RT, Idriss IM, Tokimatsu K (1986) Moduli and damping factors for dynamic analysis of cohesionless soils. *Journal of Geotechnical Engineering* 112(11):1016-1032, DOI: 10.1061/(ASCE)0733-9410(1986)112:11(1016)
Simatupang M, Okamura M (2017) Liquefaction resistance of sand remediated with carbonate precipitation at different degrees of saturation during curing. *Soils and Foundations* 57:619-631, DOI: 10.1016/j.sandf.2017.04.003
Sitharam TG, Govindaraju L (2003) Evaluation of dynamic properties of sandy soils at large strain levels. Proceedings of the work shop on current practices and future trends in earthquake geotechnical engineering, Bangalore, India, 53-60
Sreng S, Okochi Y, Kobayashi K, Tanaka H, Sugiyama H, Kusala T, Miki H, Makino M (2015) Centrifuge model tests of embankment with a new liquefaction countermeasure by ground improvement

considering constraint effect. 6th international conference on earthquake geotechnical engineering, November 1-4, Christchurch, New Zealand

Stokoe KH, Hwang SH, Lee JNK, Andrus RD (1995) Effects of various parameters on the stiffness and damping of soils at small to medium strains. *Proceedings of the international symposium on pre-failure deformation of geomaterials* 2:785-816

Suetomi I, Yoshida N (1998) Nonlinear behavior of surface deposit during the 1995 Hyogoken-Nambu earthquake. *Soils and Foundations* 38:11-22, DOI: 10.3208/sandf.38.Special_11

Teachavorasinskun S, Thongchim P, Lukkunaprasit P (2002) Shear modulus and damping of soft Bangkok clays. *Canadian Geotechnical Journal* 39:1201-1208, DOI: 10.1139/t02-048

Tsuchida H (1970) Prediction and counter measure against the liquefaction in sand deposits. Seminar in the Port and Harbour Research Institute, Ministry of Transport, Tokyo, Japan, 1-3

Tsukamoto Y, Ishihara K, Sawada S (2004) Settlement of silty sand deposits following liquefaction during earthquakes. *Soils and Foundations* 44:135-148, DOI: 10.3208/sandf.44.5_135

Vucetic M, Dobry R (1991) Effect of soil plasticity on cyclic response. *Journal of Geotechnical Engineering* 117(1):89-107, DOI: 10.1061/(ASCE)0733-9410(1991)117:1(89)

Wang Y, Gao Y, Guo L, Cai Y, Li B, Qiu Y, Mahfouz AH (2017) Cyclic response of natural soft marine clay under principal stress rotation as induced by wave loads. *Ocean Engineering* 129:191-202, DOI: 10.1016/j.oceaneng.2016.11.031

Xenaki VC, Athanasopoulos GA (2003) Liquefaction resistance of sand-mixtures: An experimental investigation of the effect of fines. *Soil Dynamics and Earthquake Engineering* 23:183-194, DOI: 10.1016/S0267-7261(02)00210-5

Yilmaz MT, Pekcan O, Bakir BS (2004) Undrained cyclic shear and deformation behaviour of silt-clay mixtures of Adapazari, Turkey. *Soil Dynamics and Earthquake Engineering* 24:497-507, DOI: 10.1016/j.soildyn.2004.04.002

Yoshida N, Sawada S, Nakamura S (2008) Simplified method in evaluating liquefaction occurrence against huge ocean trench earthquake. The 14th world conference in earthquake engineering, October 11-17, Beijing, China